Suppression, Detection and Signaling Research and Applications –

A Technical Working Conference (SUPDET 2011)

March 22-25, 2011, Orlando, FL

Liquid drainage and Flow Behavior of High Expansion (HiEx) Aqueous Fire Suppression Foams

Michael W. Conroy[1], Justin C. Taylor[2], Marcus E. Fowler[3], Peter H. Caldis[3], John P. Farley,

James W. Fleming, and Ramagopal Ananth[*]

Chemistry Division, Naval Research Laboratory, 4555 Overlook Ave., SW, Washington, DC 20375

Abstract

We have performed numerical modeling to describe drainage from a vertically rising column of HiEx, where freshly generated foam is added continuously at the top of the rising foam bed during filling. The model solves volume averaged mass and momentum balance equations to predict liquid flow through a network of channels (Plateau borders) formed by mono-dispersed bubbles with time. The model shows that the drainage rate is independent of time during filling at ambient conditions but decreases exponentially with time from a stationary foam bed during the post-filling period. Furthermore, the model shows that increasing the fill rate decreases the water loss from the foam by drainage. We also conducted experimental drainage studies on HiEx foams with initial expansion ratios of 100 to 300 using a bench-scale foam generator. The drained liquid from a rising column of foam was measured during filling and post-filling of a cylindrical vessel. The experiments show a drainage rate independent of time at a fixed fill rate followed by an exponential decay as predicted by the model. The paper will discuss the effects of bubble size, solution viscosity, and slip at the air-liquid interfaces as well as present preliminary modeling and experimental study of foam flow past an obstruction in a channel.

[1] NRC/NRL Post Doctoral Fellow

[2] NRL STEP Student

[3] NRL Student Intern

[*] Author to whom correspondence should be addressed, email: ramagopal.ananth@nrl.navy.mil

1. Introduction

The US Navy is interested in using high-expansion (HiEx) foams to suppress fires in large-volume obstructed spaces because they have very low water content (reduced weight penalty), can quickly fill obstructed areas, and are environmentally safe. HiEx is applied from the ceiling of its target space and must reach a fire with sufficient liquid content to cause extinction. After the foam is generated, liquid loss (drainage) reduces the water content of the foam and could significantly reduce its suppression ability. Drainage is a significant issue both for HiEx and low-expansion (LoEx) foams used for fighting pool fires. Further, the transport of the foam to the fire is hindered by its non-Newtonian flow behavior. Understanding drainage and flow behavior of HiEx foams is important for optimizing the technology for use by the US Navy.

The addition of freshly generated foam to the top of a rising foam bed causes its top boundary to maintain the liquid volume fraction of the injected foam. This is different from free drainage from a stagnant foam bed, wherein the liquid fraction at the top of the bed decreases very quickly with time. The addition of foam at the moving boundary can alter the drainage characteristics significantly and is not well understood. In HiEx applications, the rate of foam injection is very high (0.1 m/s), which are designed to quickly fill very large, obstructed spaces such as warehouses, aircraft hangar bays, and vehicle storage areas. HiEx foams differ significantly in structure from the more familiar LoEx foams such as aqueous film forming foam (AFFF). The drainage characteristics of HiEx foams have not been studied previously. HiEx foams typically involve large bubble sizes (about 0.01 m) and large bed height (about 3 m), which may also affect the liquid drainage rates.

LoEx foams such as AFFF are applied on to a burning hydrocarbon liquid pool at a relatively slow rate ($1x10^{-4}$ m/s) until about 0.05 m high foam bed is formed. The liquid drainage during foam application can be significant because of its high water volume fraction (0.1 to 0.2) and is also not well characterized. After the foam is applied, the stagnant foam bed is expected to provide protection against re-ignition of the pool. Therefore, it is important to understand liquid drainage both during and after the foam bed formation.

We present theoretical analysis for drainage from advancing foam as it fills a container. We will show that the liquid volume fraction decreases during the fill time. Two moving boundaries are treated in the problem: the air/foam interface where foam is added at the top, and foam/liquid interface where the foam layer is in contact with the drained liquid. The drained liquid collects beneath the foam bed and forms a liquid layer. We treat drainage after filling as a special case of the model, wherein there is a single moving boundary at the foam/liquid interface. We also perform experiments to measure liquid drainage from advancing high-expansion foams both during and after filling. The experimental data are collected at different fill rates and expansion ratios for foams used typically for fire-fighting. The foams are generated with a surfactant solution designed for HiEx fire suppression; and the foams possess greater expansion-ratio values and bubble sizes than those investigated in most previous works [1-4].

Foam rheology is an active research area, which has been mostly limited to LoEx foams. The effective viscosity of HiEx could be much different from LoEx foams because HiEx contains much less liquid, larger bubbles, and a smaller ratio of film surface area to foam volume. Further, HiEx foams spread under their own weight during large scale application. As the expansion ratio increases, the weight of the foam decreases and could cause difficulty for the foam to spread and reach behind obstructions. The effects of rheology and low density of HiEx foam on the spreading characteristics are not well understood. We provide preliminary theoretical and bench-scale experimental results for the study of HiEx foam flow in an obstructed path.

2. Foam Drainage

2.1 Drainage Theory

We consider a foam of given liquid volume fraction, α_f, injected uniformly into a vessel of height H at a constant velocity, v_{inj}. The foam surface is represented by the moving boundary, $z = h_f(t) = v_{inj}t$, where t denotes time after the start of filling. The foam is added to the top of the rising foam bed until the vessel is full. The foam is modeled as a network of dodecahedral-shaped bubbles, which contain air. The bubbles are assumed stationary with respect to a fixed observer. The liquid flows through a network of channels (Plateau borders) surrounding the bubbles inside the foam structure. Inside a channel, the liquid velocity averaged over the cross section of the channel is equivalent to the volumetric flow of liquid per unit area of channel. Each channel has its own orientation with respect to the z-direction; the average downward component of the channel velocities in the foam is v. The superficial velocity, v_s, is the volumetric flow rate of liquid flowing downward per unit cross-sectional area of the foam bed. The liquid flows down the foam column and eventually reaches the bottom of the container, where it is assumed to form a continuous liquid layer instantly. The height of the drained liquid layer is given by $z = h_w(t)$, which also marks the position of the foam/liquid interface; h_w increases with time as liquid drains.

We provide a description of the drainage behavior based on volume-averaged equations for the conservation of mass and momentum. The volume-averaged liquid fraction of the foam is defined as $\bar{\alpha}$. The time evolution of the liquid content is determined by a mass balance over the foam bed; the rate of change of the total liquid content of the foam is given by the difference in the rate of liquid addition to the foam and the rate of liquid loss from the foam column.

The liquid flow inside a channel is determined by gravity, capillary, and viscous forces acting on the liquid. We use a momentum balance over an individual channel to calculate the cross-sectional-average liquid velocity. The channel velocity is calculated with a form similar to the Hagen-Poiseuille equation for flow in a circular cylinder. Corrections are added to account

for the non-circular channel cross section, the orientation of the channel with respect to the vertical, and slip at the channel walls. We calculate a volume-averaged channel velocity, $\overline{v}$, to describe the average flow of liquid through the channels within the foam. The superficial velocity of liquid exiting the foam column is calculated from the channel velocity. It is described by Darcy's law applied to a porous medium with variable permeability characterizing the dynamics of the internal structure of the foam. The rate at which the liquid-layer height increases is equal to the superficial liquid velocity approaching the foam/liquid interface, which is given by $v_s \approx \overline{\alpha}\overline{v}$.

Important physical parameters for the drainage behavior include (A) a characteristic terminal velocity of the liquid inside a channel due to the balance of gravitational and viscous forces, equivalent to Newton's law of drag on a free falling particle, and (B) a characteristic velocity of capillary rise (per unit channel length) resulting from the balance of surface tension and viscous forces, equivalent to the liquid-rise phenomenon observed in small capillaries.

The model describes the mass and momentum balance across the entire foam bed, where h_w and $\overline{\alpha}$ are the unknowns. The model equations are solved numerically to describe drainage during filling for the parameters used in our experiments. The numerical solutions were determined by the function NDSolve (MATHEMATICA, Wolfram Research Co.).

For HiEx foam applied with relatively fast injection velocity, the approximate behavior of h_w and $\overline{\alpha}$ is given by the following analytical solutions:

$$h_w \approx \left(\frac{1}{2 + \frac{v_{inj}}{A\alpha_f}} \right) \alpha_f v_{inj} t - \frac{1}{2} \alpha_f v_{inj} t_{ind} \quad , \tag{1}$$

$$\overline{\alpha} \approx \alpha_f \left(\frac{1 + \frac{v_{inj}}{A\alpha_f}}{2 + \frac{v_{inj}}{A\alpha_f}} \right) + \frac{1}{2} \alpha_f \left(\frac{t_{ind}}{t} \right) \quad , \tag{2}$$

and

$$t_{ind} = \frac{B\left[\sqrt{\alpha_w} - \sqrt{\alpha_f}\right]}{A\alpha_f v_{inj}} = \frac{0.458\ \gamma\left[\sqrt{\alpha_w} - \sqrt{\alpha_f}\right]}{\rho_l g L \alpha_f v_{inj}} \ . \tag{3}$$

Here, t_{ind} is the induction time, the time at which drainage begins after the start of filling. The characteristic terminal velocity of the liquid in a channel is given by

$$A = \frac{\xi L^2 \rho_l g}{\mu} \quad . \tag{4}$$

Here, ξ is the permeability constant (0.0051), L is equal to the channel length (L =0.408 D_b, where D_b is the bubble diameter), ρ_l is the liquid density, g is the gravitational acceleration, μ is the liquid viscosity, and γ is the surface tension. Equation (1) shows clearly that the drained liquid is directly proportional to time and the rate of drainage is constant during filling of a container. Equation (2) indicates that the liquid fraction approaches a constant value when $t \gg$. Analytical solutions for the drainage behavior after filling indicate that the drainage rate decreases exponentially with time.

2.2 Drainage Experiments

In the experiments, we use a liquid foam solution used in the field for HiEx foam fire suppression (Buckeye HXF 2.2% High-Expansion Foam Concentrate). Foam was generated by combining liquid and air flows on a copper mesh screen. Foam exited the generator channel and traveled into a 20-L cylindrical container (height: 0.561 m, diameter: 0.213 m). The beginning of the fill time was recorded when the foam reached the base of the cylindrical container. The base of the container was formed with a sheet of aluminum foil, sloped slightly downward toward the center, where a 1-cm diameter hole allowed the drained liquid to travel out of the container. During and after the formation of the foam bed, the liquid drained from the foam was measured in a small graduated cylinder placed beneath the 1-cm diameter hole. Once the foam filled the vessel, the fill time was recorded and a plastic lid was placed on top of the vessel to minimize foam evaporation.

It was difficult to obtain bubble-size distribution inside the foam bed. We used a digital camera to take photographs of the bubbles at the free surface of the foam. We determined the bubble sizes by analyzing the photographs. The foam bubble diameters ranged from around 5 millimeter up to about 3 centimeters, with most bubbles having a diameter near one centimeter. Therefore, the foam is clearly polydisperse. We found that the theoretical predictions for liquid drained from monodisperse foam with bubble diameter of 7 mm are in excellent agreement with the experimental measurements. The predicted bubble diameter of 7 mm is close to the measured median bubble diameter.

3. Non-Newtonian Flow of Foam Around an Obstacle

Foams are known to be non-Newtonian often exhibiting yield stress. In practical applications, obstacles in the flow path pose difficulties for the foam to reach a fire hiding

behind an obstacle. Therefore, we performed bench-scale experiments and numerical simulations to understand the flow behavior of foam in an obstructed path.

3.1 Flex PDE Foam Flow Model

A non-Newtonian model is developed to describe the flow of HiEx around an obstacle in a rectangular channel. Incompressible, two-dimensional, time-dependant, Navier-Stokes equations are solved by assuming the foam as a pseudo fluid that follows Bingham-plastic stress-strain model. FlexPDE commercial software [5] is used to solve the mass and momentum conservation equations using a finite element method. A dynamic, adaptive, triangular mesh containing 800 nodes (free version of FlexPDE) is used. The geometry is very similar to the experimental set up described in the sections below. The time dependence is treated using variable order backward finite difference scheme.

In this model, the effective viscosity, μ_{eff}, of the foam was defined as

$$\mu_{eff} = \frac{\tau_0}{\gamma} + \mu_0 \quad , \tag{5}$$

where

$$\mu_0 = \frac{\alpha}{(1-\alpha)} \mu_{water} = (Ex)\, \mu_{water} \quad . \tag{6}$$

Here, μ_{water} is the viscosity of water, α is the volume fraction of gas in the foam, *Ex* is the expansion ratio of the foam, and τ_0 is the yield stress. τ_0 is given by

$$\tau_0 = \frac{0.033\sigma}{D_b}\left(\frac{\alpha^{1/3}}{(1-\alpha)^{1/4}}\right) \quad . \tag{7}$$

Also, the total shear rate, σ, is given by

$$\sigma = \sqrt{\left(\frac{\partial u}{\partial y} + \frac{\partial v}{\partial x}\right)^2 + \left(\frac{\partial u}{\partial x}\right)^2 + \left(\frac{\partial v}{\partial y}\right)^2} \quad , \tag{8}$$

where u and v are the x and y components of the velocity vector.

Equation (5) shows that μ_{eff} is a variable that approaches extremely high value when σ is zero, which represents solid-like behavior. This means that the foam resists uniform flow where there are no velocity gradients present due to the singularity in equation (5). As the foam experiences more shear its effective viscosity decreases representing fluid-like behavior. In any real flow with varying velocity gradients created by obstructions in the flow, the effective viscosity may vary by orders of magnitude across the foam. This may result in regions of high

flow and no flow. In the numerical implementation of the model, an upper limit of 300000 times the viscosity of water is imposed on μ_{eff} to avoid numerical problems due to the singularity in equation (5). The results were insensitive to this high limit on viscosity.

The yield stress is a measured quantity in separate experiments as discussed by Janiaud *et al.* [6]. Gardiner *et al.* [7] reported values of τ_0 in the dry limit, which represents a HiEx foam. They showed that τ_0 increases with the bubble diameter and the gas fraction of the foam. Therefore, the model allows us to study the effects of bubble size, gas fraction, and viscosity on the foam flow around an obstacle.

Initially, the foam is at rest and is then pushed into the channel at a pre-specified velocity. Pressure is atmospheric at channel outlet. Complete slip is assumed at the channel walls to minimize their effect on the bulk flow of foam in the channel. This will allow us to focus on the effects of the obstacle placed in the middle of the channel on foam flow. The model, however, assumes no-slip between the foam and the walls of the obstacle. (Indeed, there is small slip noticed in the experiments but is assumed negligible in the model. The result of no-slip assumption is discussed further in the experimental section.)

The simulations show significant regions of stagnant fluid in front and immediately behind the obstacle as shown in the right hand side picture of Figure 1. As one might expect, the average velocity u in x-direction (along the channel) increases as the fluid goes past the obstacle because of the reduced flow area. The simulations also show that the foam flows smoothly around the obstacle walls, and spreads into the space behind the obstacle immediately like water would. This is because equation (5) assumes that the effective viscosity (μ_{eff}) decreases at high shear rates (σ). In the region between the obstacle and the channel walls, the velocity gradients are significant, and the effective viscosity of the foam is relatively small. Future simulations will examine the effects of μ_0 and slip at the walls along with other parameters in equations (5) to (8) on the degree of spread of foam behind the obstacle.

3.2 Foam Flow Experiments

Left hand side of Figure 1 shows a rectangular channel filled with high expansion foam with a square obstacle in the middle which blocked foam movement. We built the three-dimensional rectangular channel out of acrylic plastic (36”x 16”x 5.75”) as well as a cubic obstacle, also made out of acrylic plastic (5.75”x 5.75”x 5.75”). The channel contained an opening on one end (4”x 5.75”) to fit the outlet of the foam generator, and the outlet of the channel itself was left open, with the foam flowing out into a catch pan. A removable cover split into various sections was made for access to the foam and channel before, during, and after experiments. Under the channel, we made a grid of lines every 5 cm which we used to obtain position measurements of the foam as it moved through the channel.

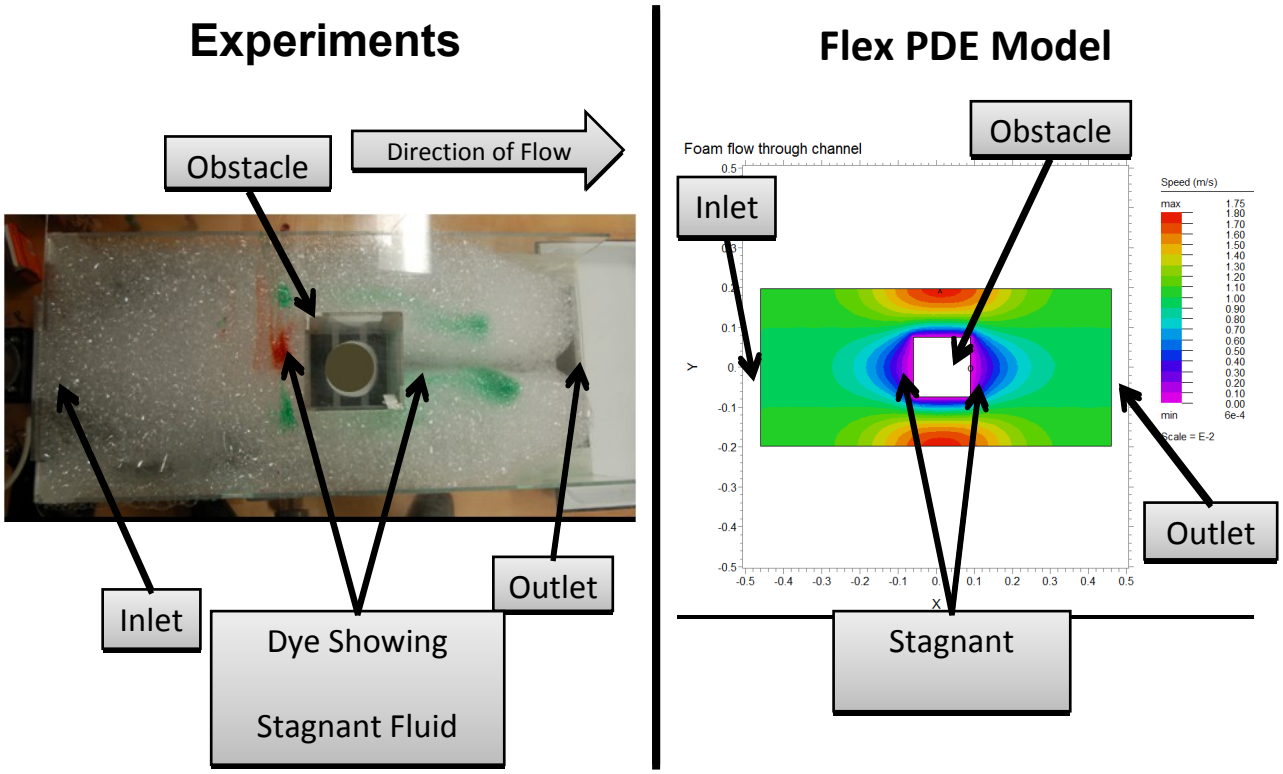

Figure 1. Comparison of FlexPDE model and experiments for non-Newtonian flow past an obstacle

We used a high expansion foam generator designed for cup burner experiments and adapted it, covering one side and forcing the foam to flow out the front of the foam chamber and into our channel. Buckeye 2.2% High Expansion Foam solution was used in the experiments, dispensed into the foam generator from a pressurized chamber. The foam was generated using a liquid flow rate of 60 mL/min and an air flow rate of 30 SLPM, with an expansion ratio between 350:1 and 400:1. We used a Tylan Flow Controller (Model: FC 262) to maintain a uniform air flow throughout the experiment.

We used drops of household food coloring (Durkee Food Colors) to dye the foam at certain points, allowing us to observe the movement of particular groups of bubbles through the channel and around the object. The dye allowed us to follow the path of the foam at various locations within the channel as well as points of zero velocity where bubbles became stationary.

After the foam generator was started and the screen inside of it primed, the channel was then covered to allow for natural foam formation and movement. Once an adequate

amount of foam had formed, part of the cover was temporarily removed and dye dropped in onto the top of the foam. The cover was then placed gently back on so that the foam could continue flowing in an enclosed space. Experiments were performed with dye being dropped in various locations within the channel. It was found that dye could only be dropped after about 30 cm of foam travel because before that point the foam was still in the process of spreading out laterally and approaching uniform forward movement. Foam was allowed to flow through the channel, around the obstacle, and out the back of the channel into a catch pan. The experiment was filmed from above so that the foam movement could be viewed later on for position measurements.

4. Results

4.1 Foam Drainage Results

We show a comparison of our model with experimental drainage measurements both during and after filling in Figure 2. The experimental data show that the height of the water layer increases linearly with time, as predicted by approximate analytical solutions for the model. During the filling process, the average liquid fraction of the foam approaches a constant value with time because the rate of liquid input balances the drainage rate; therefore, the average channel area also reaches a time-independent value. The effect of capillarity becomes relatively small as the bed height increases; the resulting balance of gravity and viscosity in the channels with fixed area causes a constant channel velocity and, therefore, a constant drainage rate.

The experimental data and model predictions for the entire drainage period including both filling and post-filling are shown in Figure 3 for the cases of Ex=183 and Ex=120. After the filling period, the drainage rate in the experiment decreases. Good agreement is also shown between the model and experiment after filling, which suggests that the data fit well to the exponential dependence of the model.

The effect of foam injection velocity on drainage is shown in Figure 4. We consider a case for very high $v_{inj}=1.1\text{x}10^{-1}$ m/s (fill time = 5 s). Figure 4 shows very little drainage during filling. We compare cases with slower injection velocities of $4.7\text{x}10^{-3}$ m/s and $9.3\text{x}10^{-4}$ m/s, corresponding to fill times of 120 s and 600 s, respectively. The curve corresponding to a 600 s fill time shows a significant drainage of liquid compared to the other two cases in Figure 4. Increasing the foam injection velocity reduces the amount of liquid drained from the foam during filling as shown in Figure 4. Note that the injection velocity, not the fill time, is the important parameter that controls drainage during filling.

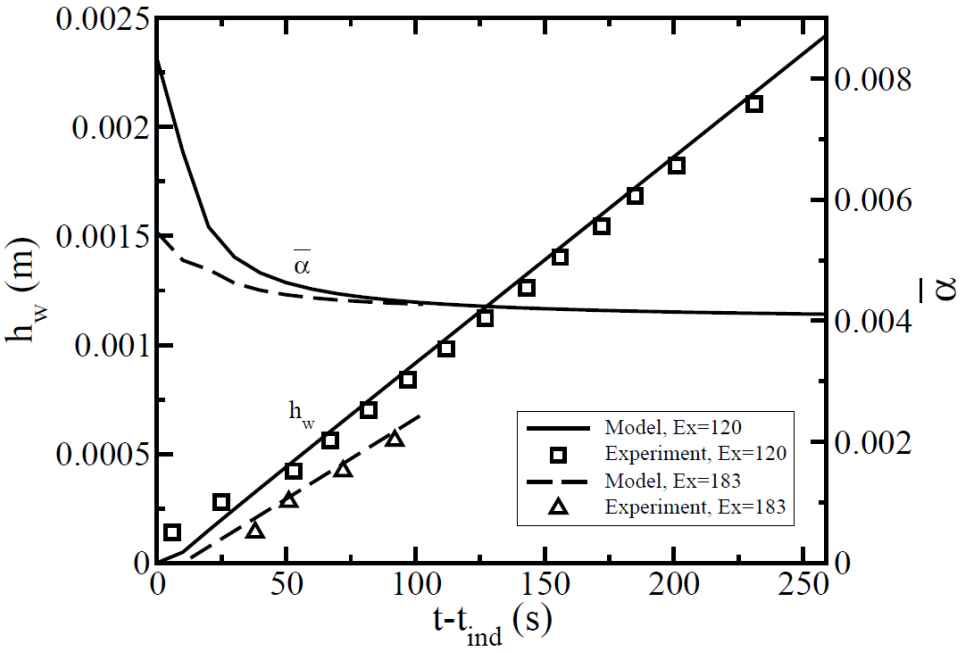

Figure 2: Comparison of model and experiment during the foam-filling period. For both cases, H=0.561 m and ξ=5.1x10^{-3}. The parameters for the case of initial Ex=120 (α_f=8.3x10^{-3}) are D_b=8x10^{-3} m, t_{fill}=259 s, v_{inj}=2.17x10^{-3} m/s, and t_{ind}=55 s. The parameters for the case of initial Ex=183 (α_f=5.5x10^{-3}) are D_b=7x10^{-3} m, t_{fill}=103 s, v_{inj}=5.45x10^{-3} m/s, and t_{ind}=15 s.

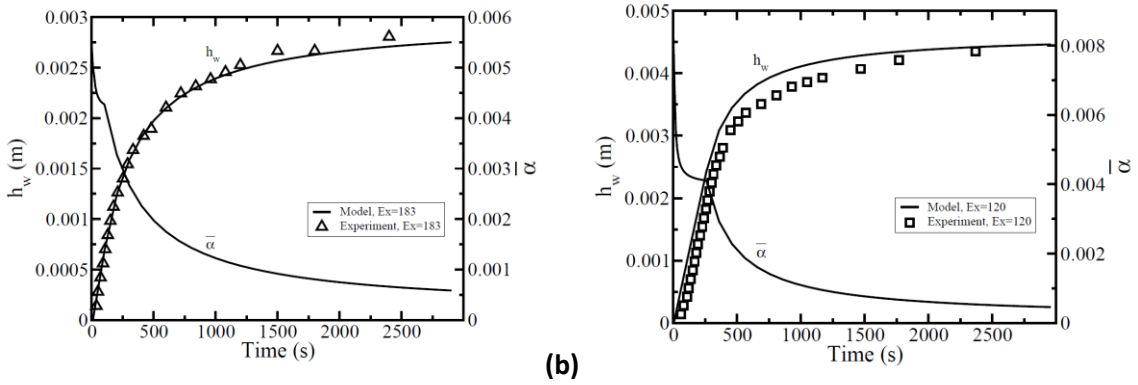

Figure 3: (a) Comparison of model predictions with experimental data for Ex= 183 (α_f=5.5x10^{-3}) during and after filling. The parameters include H=0.561 m, ξ=5.1x10^{-3} D_b=7x10^{-3} m, t_{fill}=103 s, and v_{inj}=5.45x10^{-3} m/s. (b) Comparison of model and experimental data for Ex=120 (α_f=8.3x10^{-3}) during and after filling. The parameters include H=0.561 m, ξ=5.1x10^{-3}, D_b=8x10^{-3} m, t_{fill}=259 s, v_{inj}=2.17x10^{-3} m/s.

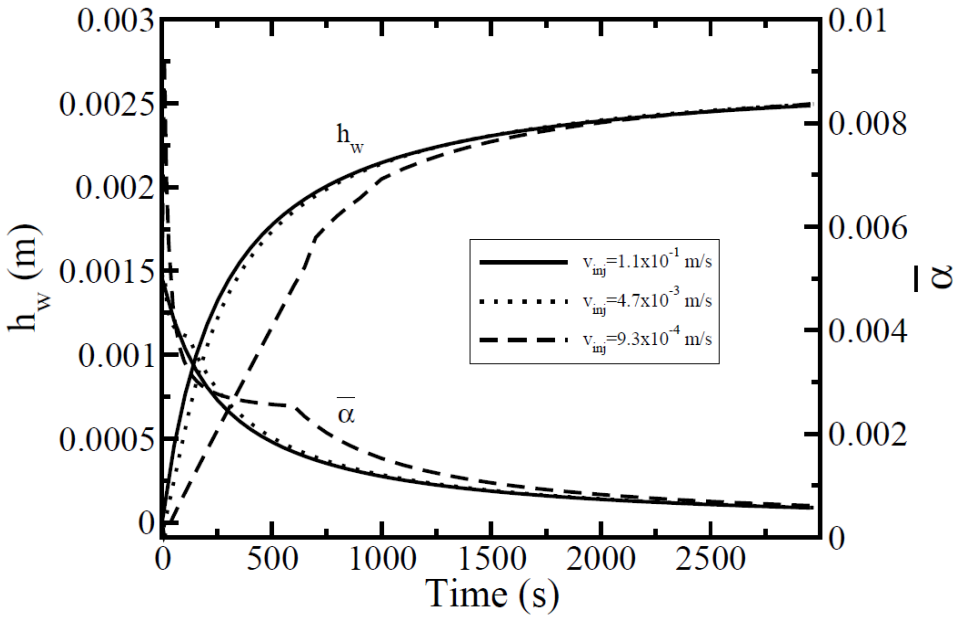

Figure 4: Model predictions for the effect of foam injection velocity on drainage. The parameters for each curve include initial Ex=200 (α_f=5x10^{-3}), H=0.561 m, ξ=6.6x10^{-3}, and D_b=6x10^{-3} m.

4.2 Foam Flow Results

The videos taken of the foam flowing through the channel were analyzed to determine foam velocity with time. As the foam traveled forward, the time was recorded each time the bubbles crossed over a line marking every 5 cm distance. The position and time data could then be used to calculate the velocity of the foam at different locations in the channel. It should be noted that since the foam went around both sides of the obstacle, the positions and times of the foam were taken on both sides as well. This data was then averaged so that trends in the overall movement in the foam as it traveled forward through the channel could be determined.

The data showed that the foam moved at a relatively constant rate of about 1.1 cm/s until it reached the obstacle. When it was forced to pass through the smaller space around the object, the velocity increased to about 1.7 cm/s. This velocity was maintained until about 5 cm past the obstacle. It was observed that the foam was moving in a formation similar to the size of the space between the obstacle and the wall until around 5 cm past the obstacle as well. After this point, the foam began to spread out more, and its velocity began to decrease until the portions of foam from either side of the obstacle came together, at which point it increased slightly and then moved forward at a relatively constant rate of about 0.8 cm/s.

Points of zero velocity were observed directly in front of and behind the obstacle. When bubbles reached the front of the obstacle, some were pushed around it, but those that encountered the obstacle in the center of its front face stopped completely and stayed in place for the duration of the experiment. A similar situation was seen at the back face of the obstacle. As the two portions of foam came together, bubbles were pushed up against the back of the obstacle, surrounding it. Once again, bubbles that encountered the face at its center stopped and did not move as other bubbles passed by.

The bubble flow described above is markedly different from that expected from a Newtonian fluid such as water. To understand the observed flow, Flex PDE model simulations were performed for the conditions used in the experiments. The Flex PDE model was used to generate theoretical velocities at various locations in the channel, which were then compared with the experimental data as shown in Figure 5. The theoretical velocities held a similar trend to what was seen in the experiment, as the foam velocity increased when the foam was forced around the obstacle and then slowed down once it had passed. It also correctly identified the regions of zero velocity directly in front of and behind the obstacle. One key difference was that the model's velocity changes were much smoother than and not as sudden as those seen in the experiment. Another difference is that the theoretical minimum and maximum velocities are closer together than the experimental velocities, and the maximum theoretical velocity of 1.53 cm/s is smaller than the maximum experimental velocity of 1.67 cm/s. Once it is past the obstacle, the theoretical velocity decreases, but is still much higher than the velocity seen in the experiment.

The key discrepancy between the two situations is the maximum and minimum velocities, as well as how quickly the foam accelerates and decelerates to those speeds. The model assumes a no-slip condition around the obstacle, meaning that the bubbles along the side of the obstacle have zero velocity. From the experiment, that was not apparent, as the bubbles were slowed down by the boundaries, yet still moved forward. It is logical to assume from the observations that there is slip along the boundaries, and that the assumption of a no-slip condition could be a source of the discrepancy between the maximum velocities, which occur in the space between the obstacle and the channel walls. It is also apparent that the model might not take into consideration the fact that after the foam passed the obstacle, it held the shape of the space between the wall and the obstacle and continued at the higher velocity for a distance of about 5 cm. Only when the foam began to spread out into the vacant space behind the obstacle did the foam velocity decrease. It is possible that the model did not correctly factor in the viscosity of the foam because it did not anticipate the bubbles holding their shape so well after the obstacle.

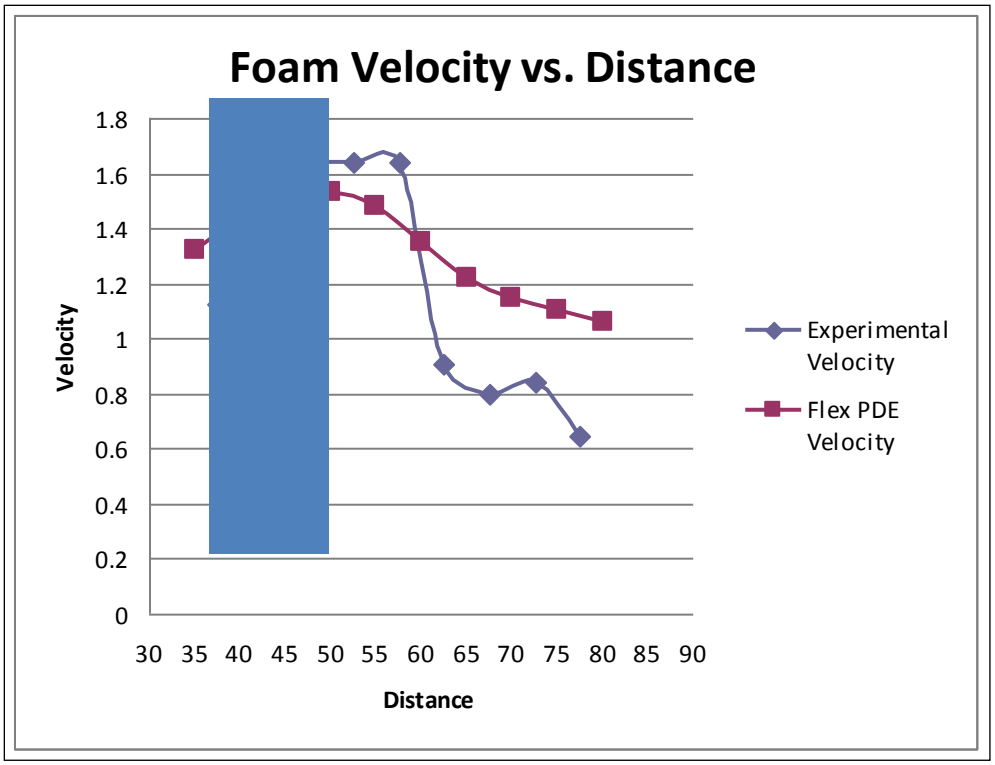

Figure 5. Experimental and theoretical (Flex PDE) foam velocities (cm/s) at different distances (cm) along the channel. The highlighted portion represents the region of the channel blocked by the obstacle. (Note: Graph only shows velocity after 30 cm.)

5. Conclusions

Model predictions indicate that liquid drains from foam at a time-independent rate as it fills a container and the drainage rate decreases exponentially after filling. Bench-scale experiments corroborate the predicted drainage behavior.

The model indicates that the amount of liquid drained from the foam during the fill time decreases with increasing injection velocity; therefore, this work suggests that increasing the foam injection velocity could reduce drainage and improve the effectiveness of HiEx foams in field applications.

Preliminary modeling and experimental results for the study of foam flow through an obstructed space indicate that stagnant regions can form in front and behind an obstacle placed in the flow path of HiEx foam.

6. Acknowledgments

This work was funded by the Office of Naval Research through the Naval Research Laboratory. This research was completed while M. W. Conroy held a National Research Council Research Associateship Award at the Naval Research Laboratory.

7. References

[1] R. A. Leonard and R. Lemlich, A Study of Interstitial Liquid Flow in Foam: Part I. Theoretical Model and Application to Foam Fractionation, American Institute of Chemical Engineers Journal 11 (1965) 18-25.

[2] D. Desai and R. Kumar, Flow Through a Plateau Border of Cellular Foam, Chemical Engineering Science 37 (1982) 1361-1370.

[3] S. Koehler, S. Hilgenfeldt, and H. A. Stone, A Generalized View of Foam Drainage: Experiment and Theory, Langmuir 16 (2000) 6327-6341.

[4] S. A. Magrabi, B. Z. Dlugogorski, and G. J. Jameson, Free Drainage in Aqueous Foams; Model and Experimental Study, American Institute of Chemical Engineers Journal 47 (2001) 314-327.

[5] FlexPDE 6, PDE Solutions Inc., (2010)

[6] E. Janiaud, D. Weaire, and S. Hutzler, “Two-Dimensional Foam Rheology with Viscous Drag”, Physical Review Letters, 97, 038302 (2006)

[7] B. S. Gardiner, B. Z. Dlugogorski, G. J. Jameson, R. P. Chhabra. Yield stress measurements of aqueous foams in the dry limit, Journal of Rheology 42 (1998) 1437-1450.